

Supporting Information

Side-chain length and dispersity in ROMP polymers with pore-generating side chains for gas separations

Francesco M. Benedetti,^{[a]‡} You-Chi Mason Wu,^{[b]‡} Sharon Lin,^{[a]‡} Yuan He,^[b] Erica Flear,^[b] Kayla R. Storme,^[b] Chao Liu,^[c] Yanchuan Zhao,^[b,c] Timothy M. Swager,^[b] and Zachary P. Smith*^[a]

[a] Department of Chemical Engineering, Massachusetts Institute of Technology, Cambridge, MA, 02139, United States

[b] Department of Chemistry, Massachusetts Institute of Technology, Cambridge, MA, 02139, United States

[c] Key Laboratory of Organofluorine Chemistry, Shanghai Institute of Organic Chemistry, Chinese Academy of Sciences, Shanghai 200032, China

‡ These authors contributed equally to this work and are co-first authors.

* E-mail: zpsmith@mit.edu

Table of Contents

Materials and methods	3
Synthetic procedures and characterization.....	4
Membrane fabrication and treatment	9
Pure-gas permeability measurements	12
CO ₂ -induced plasticization study.....	17
References.....	18

Materials and methods

Materials: Dicyclopentadiene (Alfa Aesar), sodium hydride (Sigma–Aldrich), methyl iodide (Alfa Aesar), and Grubbs 2nd-generation catalyst (Sigma–Aldrich) were purchased from commercial sources and used as received. Anhydrous dimethylformamide (DMF) was purchased from Sigma–Aldrich in SureSeal bottles and dried over 4 Å molecular sieves prior to use. Anhydrous dichloromethane (CH₂Cl₂) was obtained from an INERT PureSolv MD5 solvent purification system and stored under Ar over 4 Å molecular sieves. All other solvents were purchased at ACS grade or higher and used as received. 1,4-Anthraquinone was purified with a silica plug (using dichloromethane as the eluent) prior to use.

Silica gel chromatography: Silica gel chromatography was performed on a Biotage Isolera flash chromatography system with Biotage SNAP Ultra columns containing HP-Sphere 25µm silica.

Nuclear magnetic resonance (NMR) spectroscopy: ¹H and ¹³C NMR spectra were obtained using Bruker Avance spectrometers at 400 or 600 MHz (100 or 150 MHz) for ¹H (¹³C), in deuterated solvents as specified, and referenced to the residual solvent signal. Spectra for quantitative integration were recorded using 16 scans and 5 s relaxation time.

Size exclusion chromatography (SEC): SEC was performed in HPLC-grade tetrahydrofuran using an Agilent 1260 Infinity system with a guard column (Agilent PLgel; 5 µm; 50 x 7.5 mm) and three analytical columns (Agilent PLgel; 5µm; 300 x 7.5 mm; 10⁵, 10⁴, and 10³ Å pore sizes). The instrument was calibrated with polystyrene standards between 1.7 and 3150 kg mol⁻¹. All runs were performed at 1.0 mL min⁻¹ flow rate and 35 °C. Molecular weight values were calculated using ChemStation GPC Data Analysis Software (Rev. B.01.01) based on the refractive index signal.

Matrix-assisted laser desorption/ionization (MALDI)–time of flight (TOF) mass spectrometry (MS): MALDI–TOF MS was performed on a Bruker Autoflex Speed machine using reflector mode and positive ionization. The compound *trans*-2-[3-(4-*tert*-butylphenyl)-2-methyl-2-propenylidene]malononitrile (DCTB) was used as the matrix.

Brunauer–Emmett–Teller (BET) surface area: BET surface areas of polymer powders were measured using N₂ sorption at 77 K using a Micromeritics ASAP 2020 analyzer. Powder samples were degassed under high vacuum at 120 °C for at least 4 hours prior to analysis.

Synthetic procedures and characterization

The synthetic procedures for the OMe monomer, oligomerization, and polymerization were previously reported^{1,2} and used without modification other than the separation step. Representative procedures are presented below.

OMe oligomer: OMe monomer was added to an oven-dried Schlenk flask, which was evacuated and backfilled with Ar three times. The monomer was heated at 220 °C for 18 h.

Separation of oligomers: The oligomer mixture was separated by silica gel chromatography using a Biotage Isolera flash chromatography system. Generally, a solvent gradient of 5% to 40% EtOAc/hexanes was successful in providing sufficient separation. Retention factor (R_f) decreases with increasing n . The isolated oligomers were dissolved in a small amount of CH₂Cl₂ and precipitated in MeOH prior to polymerization in order to remove impurities, presumably from the evaporated solvent used for chromatography. OMe n -mers were dried in the vacuum oven at 60 °C for at least 3 h.

MALDI–TOS MS was used to confirm the identity and purity of the separated OMe n -mers. The observed m/z values match the expected values, as shown in **Table S1**.

Table S1. MALDI–TOF MS data and expected m/z values.

	Expected m/z	Observed m/z
OMe 2-mer	604.261	604.267
OMe 3-mer	906.392	907.415
OMe 4-mer	1208.523	1208.521
OMe 5-mer	1511.657	1511.625

In addition to MALDI (see **Figure 1c**), ^1H NMR integration ratios were used to verify the separated OMe n -mers. **Figure S1** demonstrates the method used for NMR integration, and **Table S2** shows the expected and experimentally obtained ratios.

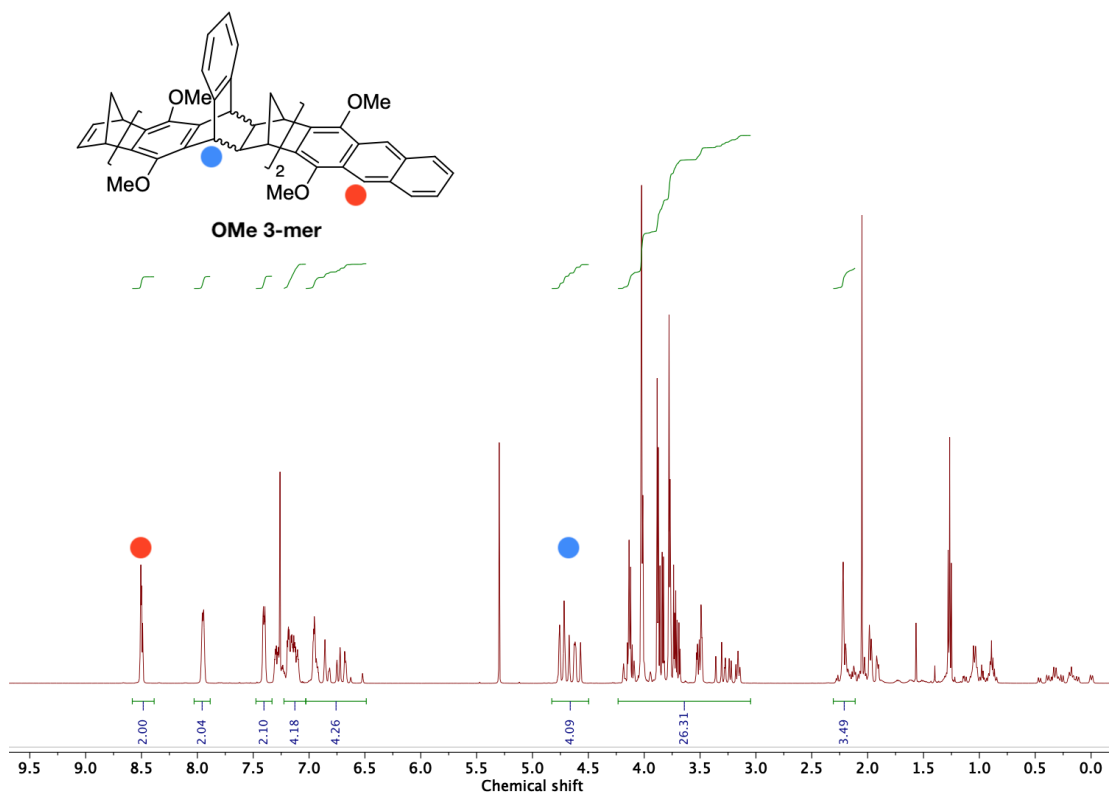


Figure S1. Example of the method used to obtain NMR integration ratios.

Table S2. NMR integration ratios of OMe *n*-mers.

	Expected ratio	Experimental ratio
OMe 2-mer	1	1.03
OMe 3-mer	2	2.05
OMe 4-mer	3	3.27
OMe 5-mer	4	4.20

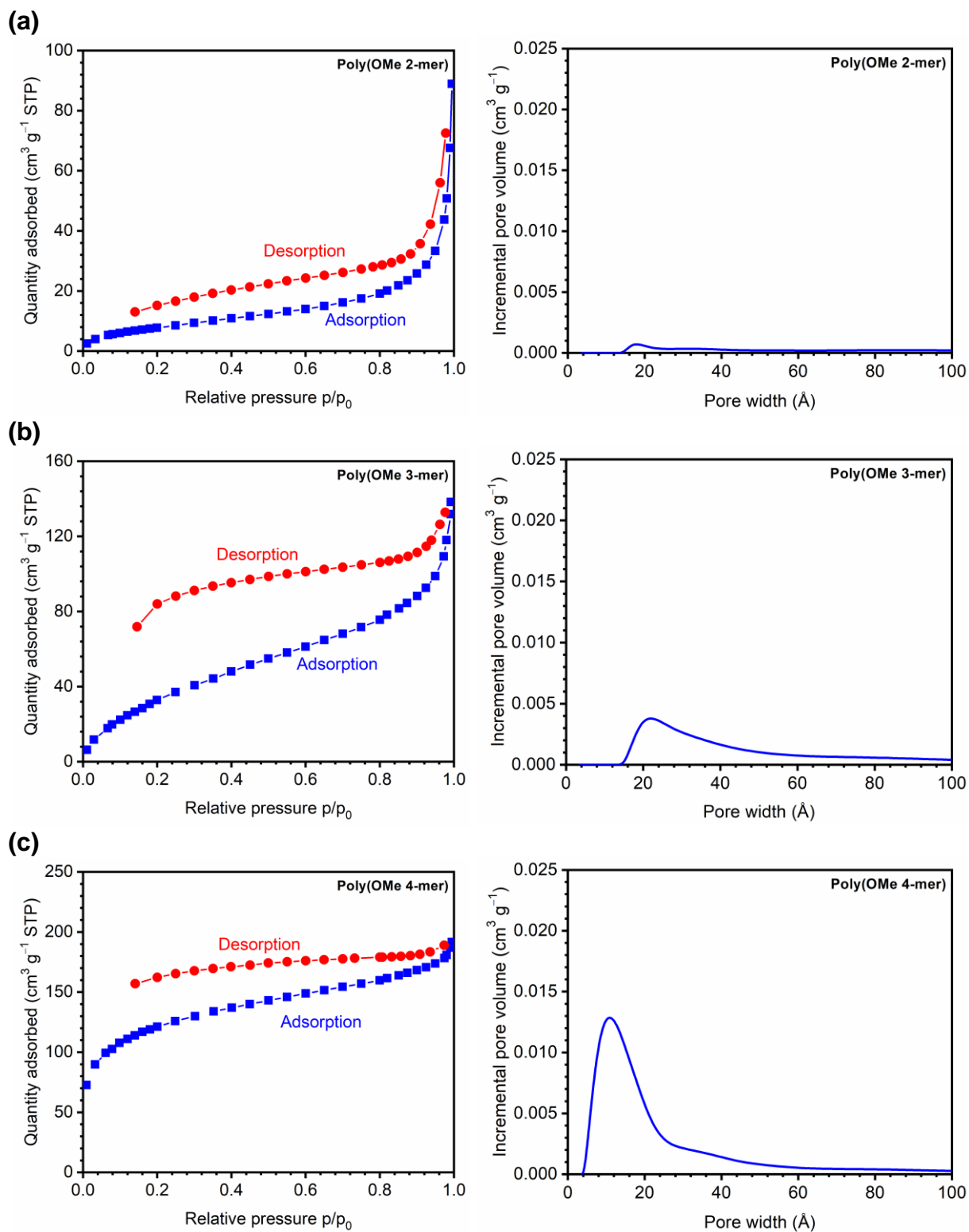
Polymerization: OMe 4-mer (168 mg, 0.14 mmol, 1 equiv.) was added to an oven-dried Schlenk flask, which was evacuated and backfilled with Ar three times, and then dissolved in CH₂Cl₂ (1 mL). In a separate oven-dried vial, Grubbs 2nd-generation catalyst (1.18 mg, 0.0014 mmol, 0.01 equiv.) was dissolved in CH₂Cl₂ (0.4 mL). The catalyst solution was transferred by syringe into the oligomer solution, and the reaction mixture was stirred at room temperature for 18 h. The flask was unsealed and 1 drop of ethyl vinyl ether was added to quench the catalyst. The polymer solution was precipitated in methanol, and the solid was collected by vacuum filtration, washed with methanol, and dried under vacuum.

Table S3. Molecular weights of poly(OMe *n*-mer)s considered in this study.

	[M]/[I]	<i>M_n</i> (kDa)	<i>D</i>
Poly(OMe 2-mer)	150	76	1.9
Poly(OMe 3-mer)	150	76	1.9
Poly(OMe 4-mer)	125	116	2.7
Poly(OMe 5-mer)	100	84	2.6

Table S4. BET surface areas of poly(OMe 2-mer) through poly(OMe 5-mer) powders. The discrepancy between the reported BET surface area of OMe-ROMP here ($484 \text{ m}^2 \text{ g}^{-1}$) and the previously reported BET surface area² ($146 \text{ m}^2 \text{ g}^{-1}$) is attributed to variation in sample preparation and measurement techniques.³

	BET Surface Area ($\text{m}^2 \text{ g}^{-1}$)
Poly(OMe 2-mer)	30
Poly(OMe 3-mer)	147
Poly(OMe 4-mer)	430
Poly(OMe 5-mer)	574
OMe-ROMP	484



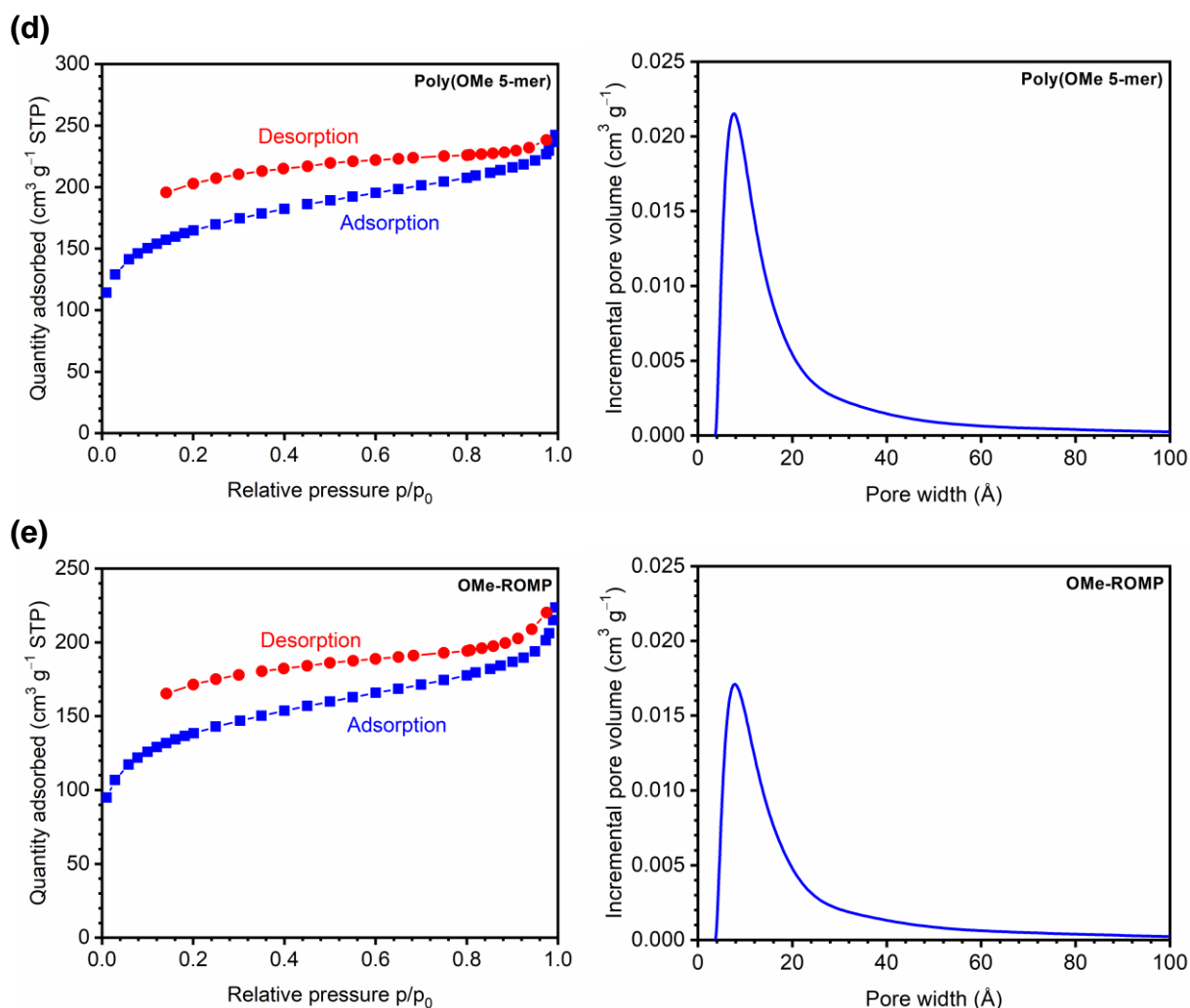


Figure S2. N₂ adsorption isotherms and pore size distributions (PSDs) calculated using the nonlocal density functional theory (NLDFT) using the standard slit carbon model of (a) poly(OMe 2-mer), (b) poly(OMe 3-mer), (c) poly(OMe 4-mer), (d) poly(OMe 5-mer), and (e) polydispersed OMe-ROMP obtained from Brunauer–Emmett–Teller (BET) analysis.

Membrane fabrication and treatment

Self-standing films of poly(OMe *n*-mer)s were made by dissolving polymers in chloroform to create ~3 wt% polymer solutions. The solutions were then cast into 50 mm diameter flat-bottom glass petri dishes that contained Norton[®] fluorinated ethylene propylene (FEP) liners (Welch

Fluorocarbon). After 4–5 days of slow evaporation at room temperature in a fumehood, stable and defect-free films were formed.

Two different treatments were employed on the self-standing films. Thermally-treated films were dried at 120 °C for 24 h under vacuum to remove residual solvent, then dried at ambient conditions for 24 h and degassed under full vacuum at 35 °C for 8 h. Alcohol-treated films were soaked in either ethanol (poly(OMe 2-mer)) or methanol (poly(OMe 3-mer) through poly(OMe 5-mer)) for 48 h. After alcohol treatment, films were air-dried in a fumehood for 24 h before testing in the permeation system.

Polymer film density for thermally-treated samples was determined using Archimedes' principle using *n*-hexane as the buoyant liquid, since the density of water was expected to be close to the sample density. Measurements were conducted using a density measurement kit from Mettler Toledo (ME-DNY-4). The fractional free volume (FFV) was then calculated for each sample using the following equation:

$$FFV = \frac{V - 1.3V_w}{V}$$

where V is the molar volume of the polymer ($\text{cm}^3 \text{mol}^{-1}$) and V_w is the van der Waals volume of the polymer ($\text{cm}^3 \text{mol}^{-1}$) determined using group contribution methods. “Method 1” refers to the method first developed by Bondi,⁴ and updated by Park and Paul⁵ in 1997 and van Krevelen⁶ in 2009 to account for larger functional groups. “Method 2” refers to the method updated by Wu et al. that accounts for new, unique structures that contain novel, contorted structural units and pendant groups that have been popularized since the first report of PIM-1 as a gas separation membrane.^{7,8}

Table S5. Density, van der Waals volumes (V_w), and fractional free volume (FFV) of poly(OMe n -mer) samples from $n = 2$ –5. “Method 1” refers to group contribution methods developed by Bondi, van Krevelen, and Park and Paul.^{4–6} “Method 2” refers to an updated group contribution method developed by Wu et al.⁷

n	Density (g cm ⁻³)	$V_{w,Method\ 1}$ (cm ³ mol ⁻¹)	$V_{w,Method\ 2}$ (cm ³ mol ⁻¹)	FFV (Method 1)	FFV (Method 2)
2	1.184 ± 0.005	362.64	325.51	0.077 ± 0.004	0.171 ± 0.004
3	1.134 ± 0.009	529.11	482.15	0.140 ± 0.007	0.216 ± 0.007
4	1.11 ± 0.02	695.58	638.79	0.17 ± 0.02	0.24 ± 0.02
5	1.12 ± 0.01	862.05	795.43	0.17 ± 0.01	0.23 ± 0.01

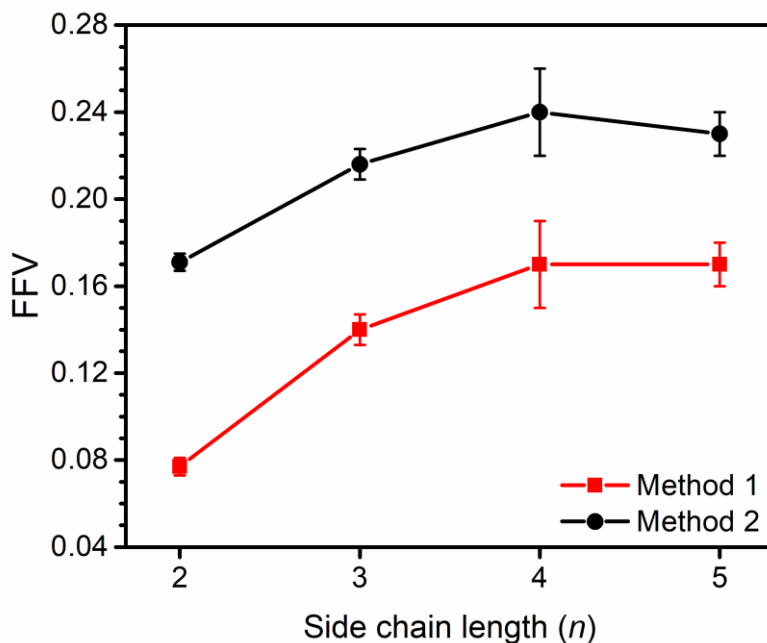


Figure S3. Fractional free volume (FFV) as a function of side-chain length (n). Red squares represent calculations using “Method 1”.^{4–6} Black circles represent calculations using “Method 2”.⁷

Pure-gas permeability measurements

Pure-gas permeability measurements of samples were performed on an automated constant-volume, variable-pressure permeation system from Maxwell Robotics. Polymer films were cut, placed on top of a hole in the center of a brass disk, and glued to the brass disk using epoxy glue (Devcon 5 min Epoxy). The glue was left to dry for at least 30 min. Afterwards, the polymer samples were sealed inside a stainless steel permeation cell (Millipore) and immersed in a water bath that was maintained at 35 °C using an immersion circulator (ThermoFisher SC150L). All gases used for testing (He, H₂, CH₄, N₂, O₂, and CO₂) were ultra-high purity from Airgas.

The permeabilities of the six aforementioned gases were determined at ~1 bar. Before testing permeation, the testing chamber was dosed with ~2 bar of helium gas to ensure that no residual gas remained in the system. Then, the samples were held under vacuum at 35 °C for 8 h. Before switching to a new permeating gas for testing, samples were again dosed with ~2 bar of helium gas and held under vacuum for at least 1 h.

Pure-gas permeability (P) was calculated using the following equation:

$$P = \frac{V_d l}{p_2 A R T} \left[\left(\frac{dp}{dt} \right)_{ss} - \left(\frac{dp}{dt} \right)_{leak} \right]$$

in which V_d is the volume downstream of the film, l is the film thickness, p_2 is the upstream pressure, A is the area of film exposed to the gas, R is the ideal gas constant, T is the absolute experimental temperature, $\left(\frac{dp}{dt} \right)_{ss}$ is the rate of pressure rise in the permeate at steady state, and $\left(\frac{dp}{dt} \right)_{leak}$ is the leak rate.⁹ The ideal gas selectivity ($\alpha_{i,j}$) was taken to be the ratio of the pure-gas permeabilities of the more permeable gas, i , to that of the less permeable gas, j (i.e., $\frac{P_i}{P_j}$). Diffusion coefficients for each gas were determined using the time-lag method, $D = \frac{l^2}{6\theta}$, in which θ is the

time lag.¹⁰ Since the diffusion coefficients for smaller gases (i.e., He and H₂) were sometimes outside of the resolution of the acquisition time of the permeation system, which is approximately 1–2 s, diffusion coefficients for these two gases are not reported. Sorption coefficients were back-calculated using the sorption–diffusion model ($S = \frac{P}{D}$).¹¹ Error bars for permeability, diffusion coefficients, and sorption coefficients were determined using the error propagation method.¹² Thicknesses of each sample are shown in **Table S6**. Aged samples, which are shown in **Table S6** with their aging times, are separate samples from “fresh” (i.e., 1 day aged) samples.

Table S6. Gas separation performance of all poly(OMe *n*-mer)s in this study. Permeability coefficients (*P*) are given in barrer (10^{-10} cm³(STP) cm cm⁻² s⁻¹ cmHg⁻¹), diffusion coefficients (*D*) are given in 10⁻⁸ cm² s⁻¹, and sorption coefficients (*S*) are given in cm³(STP) cm⁻³ atm⁻¹. All data were obtained at 35 °C and ~1 bar upstream pressure.

Polymer	Treatment		He	H ₂	N ₂	O ₂	CH ₄	CO ₂
Poly(OMe 2-mer) <i>l</i> = 91 μm	120 °C 24 h vacuum, 1 day aged	<i>P</i>	53 ± 2	80 ± 3	3.6 ± 0.1	12.7 ± 0.4	4.7 ± 0.2	83.4 ± 2.9
		<i>D</i>	/	/	3.6 ± 0.1	8.7 ± 0.2	0.91 ± 0.02	4.3 ± 0.1
		<i>S</i>	/	/	0.75 ± 0.03	1.1 ± 0.1	3.8 ± 0.2	14.7 ± 0.6
Poly(OMe 2-mer) <i>l</i> = 79 μm	EtOH treat 48 h, air-dry 24 h, 1 day aged	<i>P</i>	107 ± 3	154 ± 5	13.4 ± 0.4	33 ± 1	13.9 ± 0.4	190 ± 6
		<i>D</i>	/	/	13.1 ± 0.2	34.2 ± 1.1	4.5 ± 0.1	13.7 ± 0.2
		<i>S</i>	/	/	0.76 ± 0.03	0.73 ± 0.03	2.3 ± 0.1	10.4 ± 0.4
Poly(OMe 3-mer) <i>l</i> = 130 μm	120 °C 24 h vacuum, 1 day aged	<i>P</i>	82 ± 5	135 ± 9	5.4 ± 0.4	26.3 ± 1.7	8.5 ± 0.5	178 ± 11
		<i>D</i>	/	/	6.1 ± 0.1	20.6 ± 0.2	2.0 ± 0.1	9.9 ± 0.1
		<i>S</i>	/	/	0.7 ± 0.1	1.0 ± 0.1	3.2 ± 0.2	13.5 ± 0.9
Poly(OMe 3-mer) <i>l</i> = 91 μm	MeOH treat 48 h, air-dry 24 h, 14 days aged	<i>P</i>	169 ± 6	304 ± 11	19.0 ± 0.7	65.7 ± 2.3	28.5 ± 1.0	471 ± 17
		<i>D</i>	/	/	11.6 ± 0.3	35.4 ± 1.2	3.5 ± 0.1	18.9 ± 4.9
		<i>S</i>	/	/	1.2 ± 0.1	1.4 ± 0.1	6.1 ± 0.3	18.7 ± 0.8
Poly(OMe 4-mer) <i>l</i> = 85 μm	120 °C 24 h vacuum, 1 day aged	<i>P</i>	243 ± 10	462 ± 19	36.0 ± 1.5	112 ± 5	58.4 ± 2.4	830 ± 34
		<i>D</i>	/	/	22.3 ± 0.9	55.6 ± 3.7	6.7 ± 0.3	33.4 ± 1.6
		<i>S</i>	/	/	1.2 ± 0.1	1.5 ± 0.1	6.5 ± 0.4	18.6 ± 1.2
Poly(OMe 4-mer) <i>l</i> = 103 μm	120 °C 24 h vacuum, 34 days aged	<i>P</i>	243 ± 11	451 ± 21	34.4 ± 1.6	108 ± 5	55.6 ± 2.6	788 ± 36
		<i>D</i>	/	/	19.5 ± 1.1	49.6 ± 3.1	6.1 ± 0.4	29.8 ± 1.8
		<i>S</i>	/	/	1.3 ± 0.1	1.6 ± 0.1	6.8 ± 0.5	19.8 ± 1.5
Poly(OMe 4-mer) <i>l</i> = 82 μm	120 °C 24 h vacuum, MeOH treat 48 h, air-dry 24 h, 1 day aged	<i>P</i>	422 ± 18	839 ± 35	79.8 ± 3.3	224 ± 9	137 ± 6	1569 ± 66
		<i>D</i>	/	/	45.0 ± 1.9	96.8 ± 8.4	14.9 ± 0.3	55.8 ± 2.8
		<i>S</i>	/	/	1.3 ± 0.1	1.7 ± 0.2	6.9 ± 0.3	21.1 ± 1.4
Poly(OMe 4-mer) <i>l</i> = 94 μm	120 °C 24 h vacuum, MeOH treat 48 h, air-dry 24 h, 3 days aged	<i>P</i>	348 ± 23	717 ± 47	62.5 ± 4.1	189 ± 12	109 ± 7	1355 ± 89
		<i>D</i>	/	/	35.5 ± 3.5	89.5 ± 10.1	12.1 ± 1.1	54.0 ± 5.5
		<i>S</i>	/	/	1.3 ± 0.2	1.6 ± 0.2	6.8 ± 0.8	18.8 ± 2.3
Poly(OMe 5-mer) <i>l</i> = 82 μm	120 °C 24 h vacuum, 10 days aged	<i>P</i>	497 ± 39	1077 ± 85	107 ± 8	309 ± 24	185.1 ± 14.6	2247 ± 177
		<i>D</i>	/	/	45.5 ± 6.7	111 ± 19	16.2 ± 2.3	67.8 ± 10.4
		<i>S</i>	/	/	1.8 ± 0.3	2.1 ± 0.4	8.6 ± 1.4	24.8 ± 4.3
Poly(OMe 5-mer) <i>l</i> = 138 μm	120 °C 24 h vacuum, MeOH treat 48 h, air-dry 24 h, 1 day aged	<i>P</i>	716 ± 27	1656 ± 62	214 ± 8	552 ± 21	404 ± 15	3762 ± 141
		<i>D</i>	/	/	69.2 ± 1.6	146 ± 7	28.6 ± 0.3	81.7 ± 2.2
		<i>S</i>	/	/	2.3 ± 0.1	2.8 ± 0.2	10.6 ± 0.4	34.5 ± 1.6
Poly(OMe 5-mer) <i>l</i> = 134 μm	120 °C 24 h vacuum, MeOH treat 48 h, air-dry 24 h, 2 days aged	<i>P</i>	1076 ± 75	2476 ± 173	301 ± 21	797 ± 56	567 ± 40	5324 ± 372
		<i>D</i>	/	/	102 ± 4	203 ± 14	39.9 ± 1.0	129 ± 6
		<i>S</i>	/	/	2.3 ± 0.2	3.0 ± 0.3	10.8 ± 0.8	31.5 ± 2.6

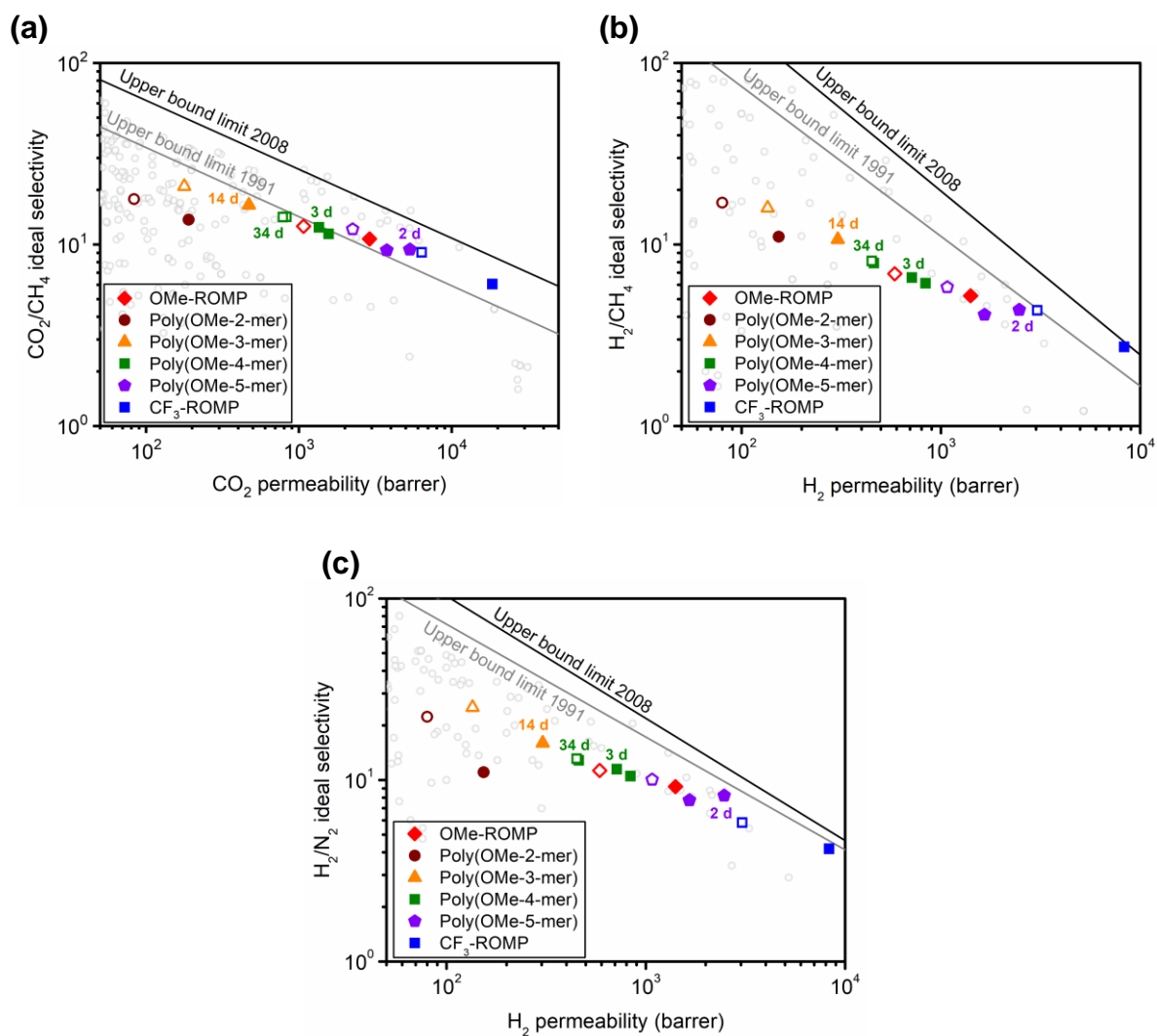


Figure S4. Robeson plots of poly(OMe *n*-mer)s, OMe-ROMP, and CF₃-ROMP for (a) CO₂/CH₄, (b) H₂/CH₄, and (c) H₂/N₂ gas pairs. Black and gray lines represent the 2008 and 1991 Robeson upper bounds, respectively.^{13,14} Filled shapes represent alcohol-treated samples, and open shapes represent thermally-treated samples.

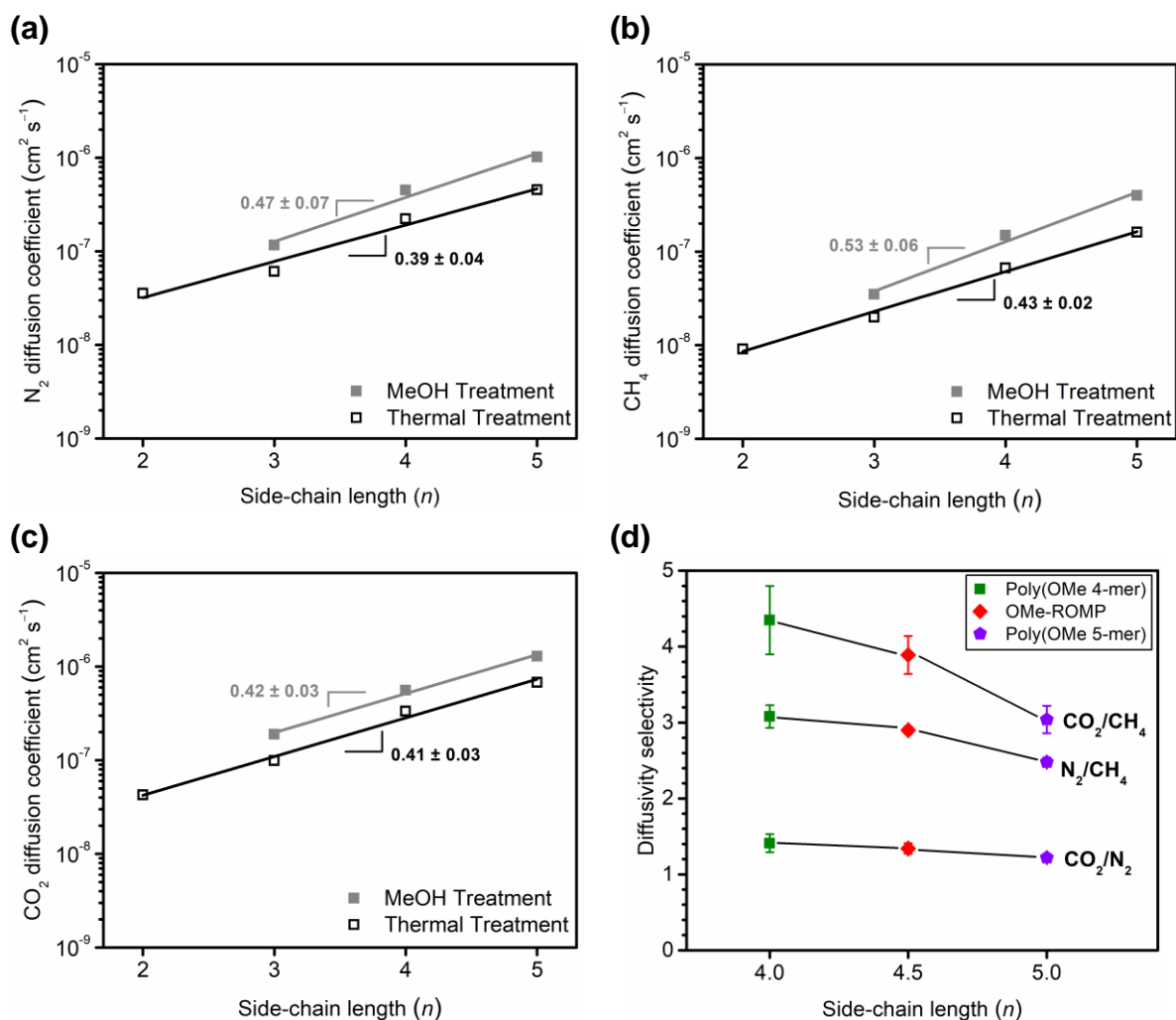


Figure S5. Diffusion coefficient for (a) N_2 , (b) CH_4 , and (c) CO_2 versus side-chain length (n). (d) Diffusivity selectivity for $n = 4$ and $n = 5$ uniform poly(OMe n -mer) and non-uniform OMe-ROMP with average $n = 4.5$ for CO_2/CH_4 , N_2/CH_4 , and CO_2/N_2 gas pairs.

Table S7. Diffusivity selectivity for fresh methanol-treated samples of poly(OMe 4-mer), OMe-ROMP (4.5 average side-chain length), and poly(OMe 5-mer).

	poly(OMe 4-mer)	OMe-ROMP (4.5 average) ²	poly(OMe 5-mer)
CO_2/CH_4	4.35 ± 0.45	3.89 ± 0.25	3.04 ± 0.18
CO_2/N_2	1.41 ± 0.12	1.34 ± 0.07	1.22 ± 0.04
O_2/N_2	2.43 ± 0.20	2.29 ± 0.15	2.06 ± 0.06
N_2/CH_4	3.08 ± 0.15	2.90 ± 0.05	2.48 ± 0.06

CO₂-induced plasticization study

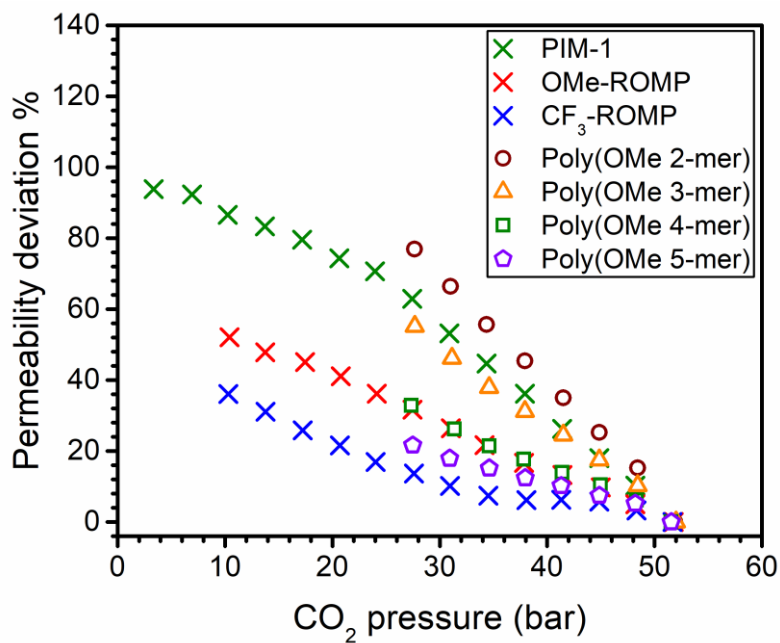


Figure S6. Hysteresis induced by conditioning of films at 51 bar of CO₂ for all samples in this study. Results for CF₃-ROMP, OMe-ROMP, and PIM-1 from our previous work² are included here for comparison.

References

- (1) Zhao, Y.; He, Y.; Swager, T. M. Porous Organic Polymers via Ring Opening Metathesis Polymerization. *ACS Macro Lett.* **2018**, *7* (3), 300–304.
- (2) He, Y.; Benedetti, F. M.; Lin, S.; Liu, C.; Zhao, Y.; Ye, H. Z.; Van Voorhis, T.; De Angelis, M. G.; Swager, T. M.; Smith, Z. P. Polymers with Side Chain Porosity for Ultraporous and Plasticization Resistant Materials for Gas Separations. *Adv. Mater.* **2019**, *31*, 1807871.
- (3) Minelli, M.; Pimentel, B. R.; Jue, M. L.; Lively, R. P.; Sarti, G. C. Analysis and Utilization of Cryogenic Sorption Isotherms for High Free Volume Glassy Polymers. *Polymer* **2019**, *170*, 157–167.
- (4) Bondi, A. Van Der Waals Volumes and Radii. *J. Phys. Chem.* **1964**, *68* (3), 441–451.
- (5) Park, J. Y.; Paul, D. R. Correlation and Prediction of Gas Permeability in Glassy Polymer Membrane Materials via a Modified Free Volume Based Group Contribution Method. *J. Membr. Sci.* **1997**, *125* (1), 23–39.
- (6) van Krevelen, D. W.; Te Nijenhuis, K. *Properties of Polymers*; Elsevier, 2009.
- (7) Wu, A. X.; Lin, S.; Mizrahi Rodriguez, K.; Benedetti, F. M.; Joo, T.; Grosz, A. F.; Storme, K. R.; Roy, N.; Syar, D.; Smith, Z. P. Revisiting Group Contribution Theory for Estimating Fractional Free Volume of Microporous Polymer Membranes. *J. Membr. Sci.* **2021**, *636*, 119526.
- (8) Budd, P. M.; Msayib, K. J.; Tattershall, C. E.; Ghanem, B. S.; Reynolds, K. J.; McKeown, N. B.; Fritsch, D. Gas Separation Membranes from Polymers of Intrinsic Microporosity. *J. Membr. Sci.* **2005**, *251* (1–2), 263–269.
- (9) Lin, H.; Freeman, B. D. 7.6 Permeation and Diffusion. In *Springer Handbook of Materials*

Measurement Methods; Czichos, H., Saito, T., Smith, L., Eds.; Springer Berlin Heidelberg: Berlin, Heidelberg, 2006.

- (10) Frisch, H. L. The Time Lag in Diffusion. *J. Phys. Chem.* **1957**, *61* (1), 93–95.
- (11) Wijmans, J. G.; Baker, R. W. The Solution-Diffusion Model: A Review. *J. Membr. Sci.* **1995**, *107* (1–2), 1–21.
- (12) Bevington, P. R.; Robinson, D. K. *Data Reduction and Error Analysis for the Physical Sciences*, 3rd ed.; McGraw-Hill: New York, 2003.
- (13) Robeson, L. M. Correlation of Separation Factor versus Permeability for Polymeric Membranes. *J. Membr. Sci.* **1991**, *62* (2), 165–185.
- (14) Robeson, L. M. The Upper Bound Revisited. *J. Membr. Sci.* **2008**, *320* (1–2), 390–400.